

Article

Tungsten Data for Current and Future Uses in Fusion and Plasma Science

Peter Beiersdorfer ^{1,*}, Joel Clementson ¹ and Ulyana I. Safronova ²

¹ Physics Department, Lawrence Livermore National Laboratory, Livermore, CA 94550, USA;
E-Mail: joel.clementson@gmail.com

² Physics Department, University of Nevada, Reno, NV 89557, USA;
E-Mail: Ulyana.I.Safronova.2@nd.edu

* Author to whom correspondence should be addressed; E-Mail: beiersdorfer1@llnl.gov

Academic Editor: James F. Babb

Received: 23 April 2015 / Accepted: 2 June 2015 / Published: 15 June 2015

Abstract: We give a brief overview of our recent experimental and theoretical work involving highly charged tungsten ions in high-temperature magnetically confined plasmas. Our work includes X-ray and extreme ultraviolet spectroscopy, state-of-the-art structure calculations, the generation of dielectronic recombination rate coefficients, collisional-radiative spectral modeling and assessments of the atomic data need for X-ray diagnostics monitoring of the parameters of the core plasma of future tokamaks, such as ITER. We give examples of our recent results in these areas.

Keywords: tungsten; X-ray spectroscopy; EUV spectroscopy; spectral modeling; atomic structure; EBIT; tokamak; ITER

1. Introduction

Atomic physics has played a very important role throughout the history of experimental plasma physics. It has been crucial for understanding the plasma energy balance and for diagnostic development [1]. With the shift in magnetic fusion research toward the very high-temperature burning plasmas expected to be found in the ITER tokamak (Latin for “the way”; but originally, an acronym for “International Tokamak Experimental Reactor”), the atomic physics of tungsten has become of high importance [2]. The reason is that tungsten will be a constituent of ITER plasmas, because of its use as a

plasma-facing component able to withstand high heat loads and with a lower tritium retention than other possible materials [3–5].

ITER diagnostics are already being developed based on using tungsten radiation. In particular, the ITER Core Imaging X-ray Spectrometer (CIXS), which is designed to measure the ion temperature and bulk plasma motion of ITER's plasma core, is being based on the X-ray emission of neon-like tungsten ions (W^{64+}) [6]. In addition, tungsten emission will be measured by extreme ultraviolet (EUV) and optical spectrometers to determine its concentration in the plasma and to assess power loss and the tungsten sputtering rate [7,8]. Moreover, tungsten is used on present-day tokamaks in preparation for ITER [9–12].

In anticipation of the importance of tungsten for fusion plasmas, our group has focused on studying the atomic properties of tungsten and its many ionization stages for over a decade. We have been doing so primarily using the Livermore electron beam ion trap facility [13], which is a device that was first designed at Livermore explicitly for studying the atomic physics of ions of heavy elements [14,15]. Our measurements have included spectral data in the X-ray region [16–23], the extreme ultraviolet regime [24–26] and the optical wavelength band [27,28].

Electron beam ion traps are now being used at a variety of international laboratories [29]. Several of these machines are being used for tungsten spectroscopy complementary to that performed on our facility. This includes measurements at the Berlin [30–32], Gaithersburg [33–35], Shanghai [36,37] and Tokyo facilities [38].

In addition to our measurements on the Livermore electron beam ion traps, we have utilized magnetic fusion plasmas to study the spectra of tungsten. These include the Sustained Spheromak Physics Experiment (SSPX), the National Spherical Torus Experiment (NSTX) and the Alcator C-mod tokamak [39–41]. We have also been involved in a significant theoretical effort utilizing some of the most advanced atomic physics computer codes [42,43].

In the past five years, our research on tungsten was shaped by our participation in the Coordinated Research Project “Spectroscopic and Collisional Data for Tungsten from 1 eV to 20 keV”, which was led by the International Atomic Energy Agency. We dubbed our effort at Livermore the “Wolfram Project”. This project has had the goal of producing experimental and theoretical data for tungsten in various spectral bands relevant to magnetic fusion research. In the following, we present an overview of the results from this effort.

2. Experimental Results

The generation of experimental spectroscopic data has been a key component in our effort. Measurements were carried out at the Livermore electron beam ion trap facility, which includes the first electron beam ion trap ever built, dubbed EBIT-I, and a high-energy version, dubbed SuperEBIT [13,44]. The spectral lines we measured during recent years were emitted by ionization stages from as low as thulium-like W^{5+} to as high as oxygen-like W^{66+} [45–47].

The Livermore electron beam ion traps have been optimized for spectroscopic measurements since their inception almost thirty years ago [48]. The electron beam ion trap is a modified electron beam ion source and built with the intent to spectroscopically study the interaction of highly charged ions

with an electron beam by looking directly into the trap. It is described in detail by Levine *et al.* [15]. In this device, the electrons pass through the 2 cm-long trap region and are compressed to a beam with a diameter of approximately 50 μm by a three-Tesla magnetic field generated by a pair of superconducting Helmholtz coils. Neutral atoms or ions with low charge are injected into the trap where they are collisionally ionized by the electron beam. The electrons can be accelerated to any energy between 0.05 keV (and lower) [49] and 200 keV (and higher) [50]. This energy is sufficient to produce any charge state of tungsten, including completely ionized tungsten W^{74+} [1]. The ions are longitudinally confined in the trap by applying the appropriate voltages to a set of three copper drift tubes through which the beam passes. Radial confinement is provided by electrostatic attraction of the electron beam, as well as flux freezing of the ions within the magnetic field. All three drift tube voltages float on top of a potential (the common drift tube voltage) that is supplied by a low-noise high-voltage amplifier, and the electron beam energy is determined by the sum of these potentials, provided the electron gun is grounded. The electron beam density is about $5 \times 10^{11} \text{ cm}^{-3}$, but can be varied [51].

Spectroscopic instrumentation includes a large variety of crystal spectrometers and grating spectrometers that cover line emission from the X-ray to the visible regime. In addition, many X-ray measurements have been made with microcalorimeters.

In Figure 1, we show the X-ray spectrum of the $3s \rightarrow 2p$ transitions of neon-like W^{64+} near 8500 eV. The figure illustrates the power of our measurement approach: new lines are observed when the energy of the electron beam is increased to allow the production of a higher ionization state. Lines from fluorine-like and oxygen-like tungsten appear as the beam energy is raised from 15 to 21 keV. The lines are absent at the lower beam energy, because the ionization potential of neon-like W^{64+} is calculated to be 15,603.6 eV, while the ionization potential of fluorine-like W^{66+} is calculated to be 15,965.5 eV [1]. L-shell X-ray transitions from tungsten ions are of special interest for the ITER tokamak, because they are under consideration as an ion temperature diagnostic of the core plasma [6].

Spectral lines from aluminum-like W^{61+} and from charge states as low as iron-like W^{48+} were observed in the ultra-soft X-ray range between 26 and 44 \AA [46]. These measurements utilized a high-resolution grating spectrometer [52] that provided a resolving power ($\lambda/\Delta\lambda \approx 1500$ to 2000) similar to that afforded by the crystal spectrometer [53] employed to make the X-ray measurements shown in Figure 1. Such a high resolving power is needed because of the high density of the $3d \rightarrow 3p$ and $3p \rightarrow 3s$ lines in this wavelength band. In fact, the large number of lines has so far precluded the identification of more than about half of the observed lines [46], which is a strong indication that more research is highly desirable.

Lines from nickel-like W^{46+} , which terminate in the closed $1s^2 2s^2 2p^6 3s^2 3p^6 3d^{10}$ shell, fall into the X-ray range near 4 to 5 \AA and are best observed with a crystal spectrometer [17,54] or an X-ray microcalorimeter [55,56]. Using the calorimeter, we were able to identify $n = 7, 6, 5, 4 \rightarrow n = 3$ transitions in nickel-like W^{46+} through selenium-like W^{40+} [23] and to assess the charge balance evolution as a function of electron energy [57].

Spectral lines from thulium-like W^{5+} , erbium-like W^{6+} and holmium-like W^{7+} were produced at very low electron beam energies (30 to 300 eV) [47]. An extended-range grazing incidence spectrometer with resolving power as high as 5000 [58] was employed to record these lines in the extreme ultraviolet wavelength range between 188 and 206 \AA [46]. The measurements enabled us to newly identify five W^{5+}

lines near 200 Å, as illustrated in Figure 2. The corresponding transitions have not yet been determined. However, we note that some of the transitions from erbium-like W^{6+} and holmium-like W^{7+} falling into this wavelength region have been identified as $5d \rightarrow 5p$ transitions [59,60].

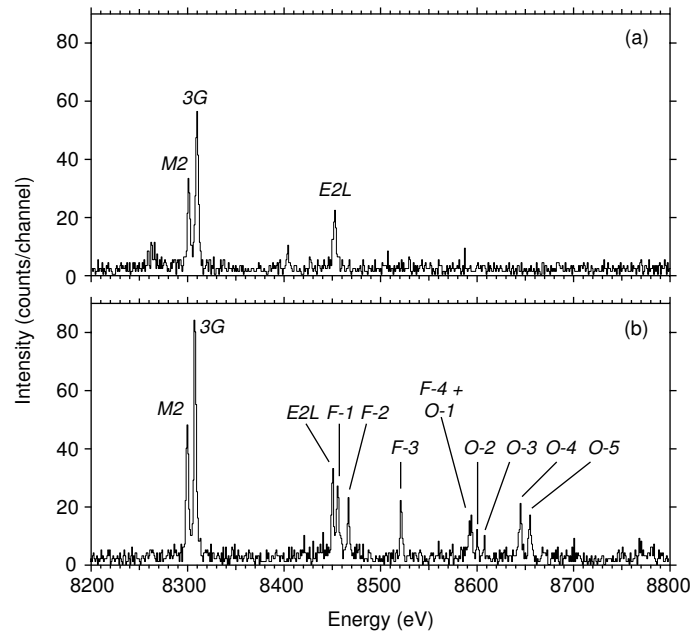


Figure 1. X-ray emission of highly charged tungsten ions at an electron beam energy of (a) 15 keV and (b) 21 keV. The strongest lines are from neon-like W^{64+} and are labeled $M2$, $3G$ and $E2L$. Lines from fluorine-like W^{65+} and oxygen-like W^{66+} are labeled by F and O , respectively.

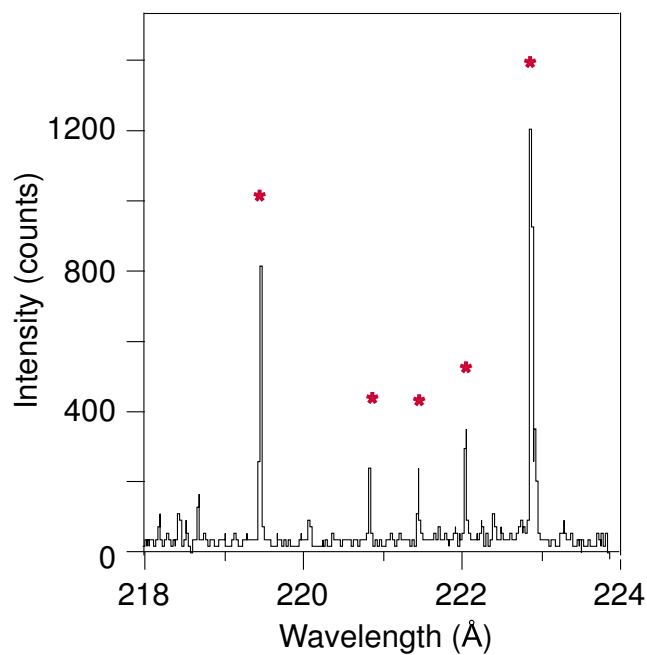


Figure 2. Emission of thulium-like W^{5+} in the extreme ultraviolet spectral band. The five lines marked with an asterisk have been newly identified.

Because several of our spectrometers have been installed on magnetic fusion devices in the United States [61–66], we can obtain tungsten spectra also from these sources, provided that tungsten is introduced into these machines. One such spectrum is shown in Figure 3. It was obtained on the Alcator C-mod tokamak at the Massachusetts Institute of Technology [67] and shows bright tungsten emission near 50 Å. Comparison with spectral data from other fusion machines, notably from the Large Helical Device in Japan [68], points to charge states silver-like W^{27+} , palladium-like W^{28+} and ruthenium-like W^{29+} as the strongest emitters, as described by Podpaly *et al.* [67].

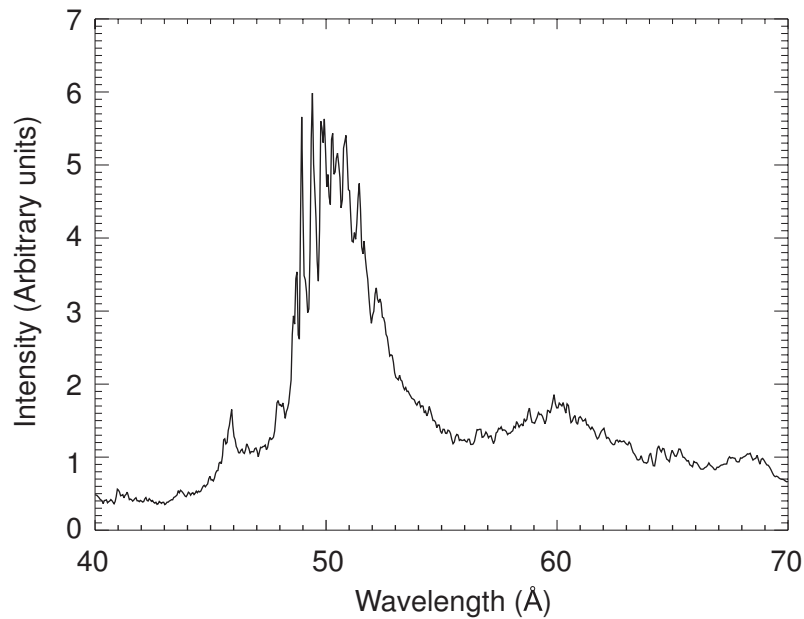


Figure 3. Emission from tungsten ions observed on the Alcator C-mod tokamak.

3. Theoretical Atomic Data and Spectral Modeling

Our Wolfram project includes a significant collisional-radiative modeling effort using atomic data that we have generated with the Flexible Atomic Code (FAC) developed by Gu [69]. For example, we have generated modeled spectra of the $n = 3 \rightarrow n = 2$ X-ray transitions of near neon-like tungsten ions (W^{56+} to W^{71+}) [2]. In addition, we have performed such modeling for essentially all of the ionization stages we investigated experimentally, and the results can be found in our papers mentioned above.

In Figure 4, we show a spectrum predicted by our modeling calculations for vanadium-like W^{51+} in the 1000 to 4000 eV X-ray range. This was part of a large effort that produced theoretical spectral data from germanium-like W^{42+} through vanadium-like W^{51+} [70].

Our collisional-radiative modeling effort has been augmented with calculations of the ionization potentials of all tungsten ions [1], as well as specific atomic parameters needed for spectral measurements and diagnostics. The latter calculations include energy levels, radiative rates, oscillator strengths and autoionization rates. We employed three very different atomic physics computer codes, *i.e.*, the Hartree–Fock-relativistic method (COWAN code), the multi-configuration relativistic Hebrew University–Lawrence Livermore Atomic Code (HULLAC code) and the relativistic many-body perturbation theory method (RMBPT code) [71–77], in order to estimate the reliability of the calculations from the spread of the obtained results.

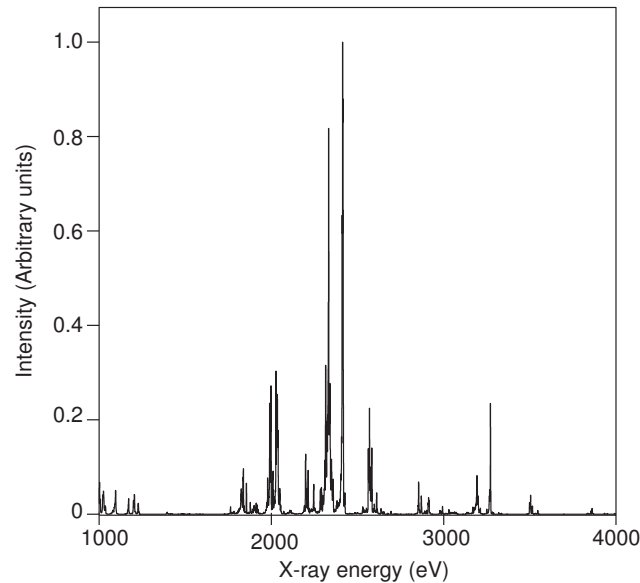


Figure 4. Spectral emission of vanadium-like W^{51+} in the 1000 to 4000 eV X-ray range predicted by calculations performed with the Flexible Atomic Code.

In Figure 5, we show the total dielectronic recombination rate coefficients we have calculated as a function of electron temperature for the recombination of neon-like W^{64+} , sodium-like W^{63+} and copper-like W^{45+} into their respective next lower ionization states. In all cases, it is assumed that the recombining ion is in its ground state. Because the ground state of neon-like W^{64+} is a completely closed shell, there are no low-energy dielectronic resonances. As a consequence, the dielectronic recombination rate vanishes as the electron temperature drops below 100 eV. By contrast, the ground state of both sodium-like and copper-like tungsten has a single valence electron outside an otherwise closed shell. This allows for low-energy resonances that contribute to the total recombination rate coefficient, even at very low plasma temperatures, as shown by the figure.

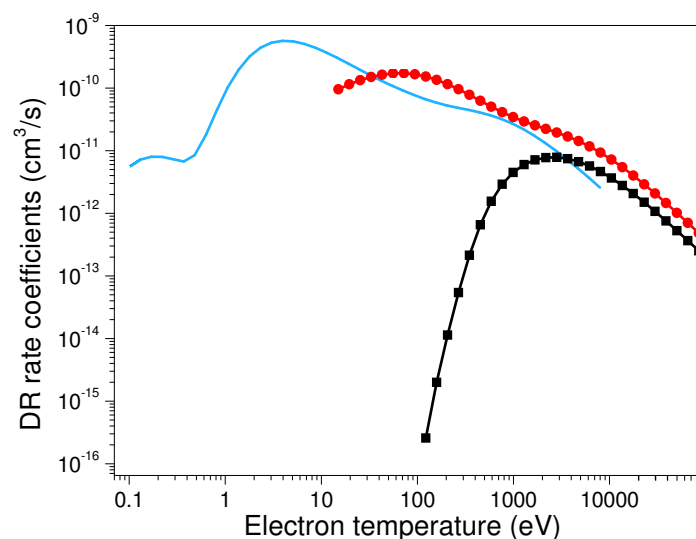


Figure 5. Total dielectronic recombination rate coefficients for neon-like W^{64+} (black trace with solid squares), sodium-like W^{63+} (red trace with solid circles) and copper-like W^{45+} (light blue trace) recombining into their respective next lower ionization state.

4. Assessment of Atomic Data Needs for ITER Core Diagnostics

Tungsten radiation will be observed on ITER with a variety of instrumentation. For example, various survey-type instruments will monitor plasma performance near the plasma edge [7,78], where lower ionization stages of tungsten will radiate. The core plasma will be monitored with the aforementioned CIXS instrument [6] and possibly an X-ray microcalorimeter [79]. Both of these instruments are designed to determine the ion temperature from the L-shell emission of tungsten ions.

Recently, we have compiled specific atomic data needs to increase the reliability of the core ITER X-ray diagnostics [80,81]. These include: (1) absolute wavelength measurements with accuracy lines on the order of about 0.02 eV of the L-shell lines of neon-like W^{64+} and of the neighboring sodium-like and fluorine-like tungsten lines; (2) measurements and calculations of the position and intensity of the dielectronic satellite lines associated with the neon-like W^{64+} lines, including those with a spectator electron in a high principal quantum number; and (3) calculation and measurement of the excitation rates at a level of accuracy of about 5%, including excitation by indirect processes [82], such as resonance excitation and cascade contributions.

There is also a growing need for reliable ionization balance calculations, which for tungsten is a nontrivial undertaking [83]. The reason for this need is that the CIXS will provide radial profiles of the ion abundance in ITER. When compared to accurate ionization balance calculations, such radial profile measurements can be used to extract the ion transport parameters, *i.e.*, the radial ion diffusion coefficient and the inward pinch velocities, as detailed recently by Beiersdorfer [81]. Diagnosing transport and ultimately controlling it is a prime objective in fusion research, and reliable atomic physics is a prerequisite for using the CIXS in this endeavor.

Acknowledgments

This work was performed under the auspices of the U. S. Department of Energy by Lawrence Livermore National Laboratory under Contract DE-AC52-07NA27344 and was carried out in support of the International Atomic Energy Agency Coordinated Research Project “Spectroscopic and Collisional Data for Tungsten from 1 eV to 20 keV”.

Author Contributions

All three authors have substantially contributed to the physics presented in this article. All authors have read and approved the final manuscript.

Conflicts of Interest

The authors declare no conflict of interest.

References

1. Beiersdorfer, P.; May, M.J.; Scofield, J.H.; Hansen, S.B. Atomic physics and ionization balance of high-Z ions: Critical ingredients for characterizing and understanding high-temperature plasmas. *High Energ. Dens. Phys.* **2012**, *8*, 271–283.

2. Clementson, J.; Beiersdorfer, P.; Lennartsson, T. Atomic data of tungsten for current and future uses in fusion and plasma science. *AIP Conf. Proc.* **2013**, *1525*, 78–83.
3. Bolt, H.; Barabash, V.; Federici, G.; Linke, J.; Loarte, A.; Roth, J.; Sato, K. Plasma facing and high heat flux materials—Needs for ITER and beyond. *J. Nucl. Mater.* **2002**, *307*, 43–52.
4. Skinner, C.H. Applications of EBIT to magnetic fusion diagnostics. *Can. J. Phys.* **2008**, *86*, 285–290.
5. Peacock, N.J.; O’Mullane, M.G.; Barnsley, R.; Tarbutt, M.R. Anticipated X-ray and VUV spectroscopic data from ITER with appropriate diagnostic instrumentation. *Can. J. Phys.* **2008**, *86*, 277–284.
6. Beiersdorfer, P.; Clementson, J.; Dunn, J.; Gu, M.F.; Morris, K.; Podpaly, Y.; Wang, E.; Bitter, M.; Feder, R.; Hill, K.W.; *et al.* The ITER core imaging X-ray spectrometer. *J. Phys. B* **2010**, *43*, 144008.
7. Varshney, S.K.; Barnsley, R.; O’Mullane, M.G.; Jakhar, S. Bragg X-ray survey spectrometer for ITER. *Rev. Sci. Instrum.* **2012**, *83*, 10E126.
8. Seon, C.R.; Hong, J.H.; Jang, J.; Lee, S.H.; Choe, W.; Lee, H.H.; Cheon, M.S.; Pak, S.; Lee, H.G.; Biel, W.; *et al.* Test of prototype ITER vacuum ultraviolet spectrometer and its application to impurity study in KSTAR plasmas. *Rev. Sci. Instrum.* **2014**, *85*, 11E403.
9. Matthews, G.F.; Edwards, P.; Hirai, T.; Kear, M.; Lioure, A.; Lomas, P.; Loving, A.; Lungu, C.; Maier, H.; Mertens, P.; Neilson, D.; *et al.* Overview of the ITER-like wall project. *Phys. Scr.* **2007**, *T128*, 137–143.
10. Sips, A.C.C.; Gruber, O.; ASDEX Upgrade Team. Compatibility of ITER scenarios with an all-W wall. *Plasma Phys. Controll. Fusion* **2008**, *50*, 124028.
11. Neu, R.; Bobkov, V.; Dux, R.; Fuchs, J.C.; Gruber, O.; Herrmann, A.; Kallenbach, A.; Maier, H.; Mayer, M.; Rohde, V.; *et al.* Ten years of W programme in ASDEX Upgrade—Challenges and conclusions. *Phys. Scr.* **2009**, *T138*, 014038.
12. Li, J.; Luo, G.; Ding, R.; Yao, D.; Chen, J.; Cao, L.; Hu, J.; Li, Q.; the EAST Team. Plasma facing components for the Experimental Advanced Superconducting Tokamak and CFETR. *Phys. Scr.* **2014**, *T159*, 014001.
13. Beiersdorfer, P. A “brief” history of spectroscopy on EBIT. *Can. J. Phys.* **2008**, *86*, 1–10.
14. Marrs, R.E.; Levine, M.A.; Knapp, D.A.; Henderson, J.R. Measurement of electron-impact-excitation cross sections for very highly charged ions. *Phys. Rev. Lett.* **1988**, *60*, 1715–1718.
15. Levine, M.A.; Marrs, R.E.; Bardsley, J.N.; Beiersdorfer, P.; Bennett, C.L.; Chen, M.H.; Cowan, T.; Dietrich, D.; Henderson, J.R.; Knapp, D.A.; *et al.* The use of an electron beam ion trap in the study of highly charged ions. *Nucl. Instrum. Methods* **1989**, *B43*, 431–440.
16. Elliott, S.R.; Beiersdorfer, P.; MacGowan, B.J.; Nilsen, J. Measurements of line overlap for resonant spoiling of X-ray lasing transitions in nickel-like tungsten. *Phys. Rev. A* **1995**, *52*, 2689–2692.
17. Neill, P.; Harris, C.; Safronova, A.; Hamasha, S.; Hansen, S.; Safronova, U.; Beiersdorfer, P. The study of X-ray M-shell spectra of W ions from the Lawrence Livermore National Laboratory Electron Beam Ion Trap. *Can. J. Phys.* **2004**, *82*, 931–942.

18. Shlyaptseva, A.; Fedin, D.; Hamasha, S.; Harris, C.; Kantsyrev, V.; Neill, P.; Quart, N.; Safronova, U.I.; Beiersdorfer, P.; Boyce, K.; *et al.* Development of M-shell X-ray spectroscopy and spectropolarimetry of z-pinch tungsten plasmas. *Rev. Sci. Instrum.* **2004**, *75*, 3750–3752.
19. Osborne, G.C.; Safronova, A.S.; Kantsyrev, V.L.; Safronova, U.I.; Yilmaz, M.F.; Williamson, K.; Shrestha, I.; Beiersdorfer, P. Diagnostic of charge balance in high-temperature tungsten plasmas using LLNL EBIT. *Rev. Sci. Instrum.* **2008**, *79*, 10E308.
20. Podpaly, Y.; Clementson, J.; Beiersdorfer, P.; Williamson, J.; Brown, G.V.; Gu, M.F. Spectroscopy of $2s_{1/2} - 2p_{3/2}$ transitions in W^{65+} through W^{71+} . *Phys. Rev. A* **2009**, *80*, 052504.
21. Clementson, J.; Beiersdorfer, P.; Gu, M.F. X-ray spectroscopy of E2 and M3 transitions in Ni-like W. *Phys. Rev. A* **2010**, *81*, 012505.
22. Clementson, J.; Beiersdorfer, P. Wavelength measurement of $n = 3$ to $n = 3$ transitions in highly charged tungsten ions. *Phys. Rev. A* **2010**, *81*, 052509.
23. Clementson, J.; Beiersdorfer, P.; Brown, G.V.; Gu, M.F. Spectroscopy of M-shell x-ray transitions in Zn-like through Co-like W. *Phys. Scr.* **2010**, *81*, 015301.
24. Utter, S.B.; Beiersdorfer, P.; Träbert, E. Electron-beam ion-trap spectra of tungsten in the EUV. *Can. J. Phys.* **2002**, *80*, 1503–1515.
25. Utter, S.B.; Beiersdorfer, P.; Träbert, E.; Clothiaux, E.J. Wavelengths of the $4s_{1/2} - 4p_{3/2}$ resonance lines in Cu-like heavy ions. *Phys. Rev. A* **2003**, *67*, 032502.
26. Utter, S.B.; Beiersdorfer, P.; Träbert, E. Accurate wavelengths of resonance lines in Zn-like heavy ions. *Can. J. Phys.* **2003**, *81*, 911–918.
27. Utter, S.B.; Beiersdorfer, P.; Brown, G.V. Measurement of an unusual M1 transition in the ground state of Ti-like W^{52+} . *Phys. Rev. A* **2000**, *61*, 030503.
28. Utter, S.B.; Beiersdorfer, P.; Träbert, E. Wavelength measurement of the prominent M1 transition in the ground state of Ti-like Pt, Au, and Tl ions. *Phys. Rev. A* **2003**, *67*, 012508.
29. Beiersdorfer, P. Spectroscopy with trapped highly charged ions. *Phys. Scr.* **2009**, *T134*, 014010.
30. Radtke, R.; Biedermann, C.; Schwob, J.L.; Mandelbaum, P.; Doron, R. Line and band emission from tungsten ions with charge 21+ to 45+ in the 45–70 Å range. *Phys. Rev. A* **2001**, *64*, 012720.
31. Hutton, R.; Zou, Y.; Reyna Almandos, J.; Biedermann, C.; Radtke, R.; Greier, A.; Neu, R. EBIT spectroscopy of Pm-like tungsten. *Nucl. Instrum. Methods Phys. Res. B* **2003**, *205*, 114–118.
32. Radtke, R.; Biedermann, C.; Mandelbaum, P.; Schwob, J.L. X-ray and EUV spectroscopic measurements of highly charged tungsten ions relevant to fusion plasmas. *J. Phys. Conf. Ser.* **2007**, *58*, 113.
33. Ralchenko, Y.; Reader, J.; Pomeroy, J.M.; Tan, J.N.; Gillaspay, J.D. Spectra of W^{39+} W^{47+} in the 1220 nm region observed with an EBIT light source. *J. Phys. B* **2007**, *40*, 3861–3875.
34. Ralchenko, Y.; Draganic, I.N.; Tan, J.N.; Gillaspay, J.D.; Pomeroy, J.M.; Reader, J.; Feldman, U.; Holland, G.E. EUV spectra of highly-charged ions W^{54+} W^{63+} relevant to ITER diagnostics. *J. Phys. B* **2008**, *41*, 021003.
35. Ralchenko, Y.; Draganić, I.N.; Osin, D.; Gillaspay, J.D.; Reader, J. Spectroscopy of diagnostically important magnetic-dipole lines in highly charged $3d^n$ ions of tungsten. *Phys. Rev. A* **2011**, *83*, 032517.

36. Fei, Z.; Zhao, R.; Shi, Z.; Xiao, J.; Qiu, M.; Grumer, J.; Andersson, M.; Brage, T.; Hutton, R.; Zou, Y. Experimental and theoretical study of the ground-state M1 transition in Ag-like tungsten. *Phys. Rev. A* **2012**, *86*, 062501.
37. Fei, Z.; Li, W.; Grumer, J.; Shi, Z.; Zhao, R.; Brage, T.; Huldt, S.; Yao, K.; Hutton, R.; Zou, Y. Forbidden-line spectroscopy of the ground-state configuration of Cd-like W. *Phys. Rev. A* **2014**, *90*, 052517.
38. Watanabe, H.; Nakamura, N.; Kato, D.; Sakaue, H.A.; Ohtani, S. Lines from highly charged tungsten ions observed in the visible region between 340 and 400 nm. *Can. J. Phys.* **2012**, *90*, 497–501.
39. Clementson, J.; Beiersdorfer, P.; Magee, E.W.; McLean, H.S.; Wood, R.D. Tungsten spectroscopy relevant to the diagnostics of ITER divertor plasmas. *J. Phys. B* **2010**, *43*, 144009.
40. Clementson, J.; Beiersdorfer, P.; Roquemore, A.L.; Skinner, C.H.; Mansfield, D.K.; Hartzfeld, K.; Lepson, J.K. Experimental setup for tungsten transport studies at the NSTX tokamak. *Rev. Sci. Instrum.* **2010**, *81*, 10E326.
41. Reinke, M.L.; Beiersdorfer, P.; Howard, N.T.; Magee, E.W.; Podpaly, Y.; Rice, J.E.; Terry, J.L. Vacuum ultraviolet impurity spectroscopy on the Alcator C-Mod tokamak. *Rev. Sci. Instrum.* **2010**, *81*, 10D736.
42. Safronova, U.I.; Safronova, A.S.; Beiersdorfer, P. Excitation energies, radiative and autoionization rates, dielectronic satellite lines, and dielectronic recombination rates for excited states of Na-like W from Ne-like W. *At. Data Nucl. Data Tables* **2009**, *95*, 751–785.
43. Safronova, U.I.; Safronova, A.S.; Beiersdorfer, P. Excitation energies, radiative and autoionization rates, dielectronic satellite lines and dielectronic recombination rates for excited states of Mg-like W from Na-like W. *J. Phys. B* **2009**, *42*, 165010.
44. Beiersdorfer, P.; Behar, E.; Boyce, K. R.; Brown, G. V.; Chen, H.; Gendreau, K. C.; Graf, A.; Gu, M.-F.; Harris, C. L.; Kahn, S. M.; Kelley, R. L.; Lepson, J. K.; May, M. J.; Neill, P. A.; Pinnington, E. H.; Porter, F. S.; Smith, A. J.; Stahle, C. K.; Szymkowiak, A. E.; Tillotson, A.; Thorn, D. B.; Träbert, E.; Wargelin, B. J. Overview of the Livermore electron beam ion trap project. *Nucl. Instrum. Methods* **2003**, *205*, 173–177.
45. Beiersdorfer, P.; Lepson, J.K.; Schneider, M.B.; Bode, M.P. L-shell X-ray Emission from neon-like W^{64+} . *Phys. Rev. A* **2012**, *86*, 012509.
46. Lennartsson, T.; Clementson, J.; Beiersdorfer, P. Experimental wavelengths for intrashell transitions in tungsten ions with partially filled 3p and 3d subshells. *Phys. Rev. A* **2013**, *87*, 062505.
47. Clementson, J.; Lennartsson, T.; Beiersdorfer, P.; Safronova, A.S. Extreme Ultraviolet Spectra of Few-times Ionized Tungsten for Divertor Plasma Diagnostics. *Atoms* **2015**, submitted.
48. Marrs, R.E. Milestones in EBIT spectroscopy and why it almost did not work. *Can. J. Phys.* **2008**, *86*, 11–18.
49. Lepson, J.K.; Beiersdorfer, P. Low-energy operation of the Lawrence Livermore electron beam ion traps: Atomic spectroscopy of Si V, S VII and Ar IX. *Phys. Scr.* **2005**, *2005*, 62.
50. Marrs, R.E.; Elliott, S.R.; Knapp, D.A. Production and trapping of hydrogenlike and bare uranium ions in an electron beam ion trap. *Phys. Rev. Lett.* **1994**, *72*, 4082–4085.

51. Chen, H.; Beiersdorfer, P.; Heeter, L.A.; Liedahl, D.A.; Naranjo-Rivera, K.L.; Träbert, E.; Gu, M.F.; Lepson, J.K. Experimental and theoretical evaluation of density-sensitive N VI, Ar XIV, and Fe XXII line ratios. *Astrophys. J.* **2004**, *611*, 598.
52. Beiersdorfer, P.; Magee, E.W.; Träbert, E.; Chen, H.; Lepson, J.K.; Gu, M.F.; Schmidt, M. Flat-field grating spectrometer for high-resolution soft X-ray and extreme ultraviolet measurements on an electron beam ion trap. *Rev. Sci. Instrum.* **2004**, *75*, doi:10.1063/1.1779609.
53. Beiersdorfer, P.; Marrs, R.E.; Henderson, J.R.; Knapp, D.A.; Levine, M.A.; Platt, D.B.; Schneider, M.B.; Vogel, D.A.; Wong, K.L. High-resolution X-ray spectrometer for an electron beam ion trap. *Rev. Sci. Instrum.* **1990**, *61*, 2338–2342.
54. Brown, G.V.; Beiersdorfer, P.; Widmann, K. Wide-band, high-resolution soft X-ray spectrometer for the Electron Beam Ion Trap. *Rev. Sci. Instrum.* **1999**, *70*, 280–283.
55. Porter, F.S.; Brown, G.V.; Boyce, K.R.; Kelley, R.L.; Kilbourne, C.A.; Beiersdorfer, P.; Chen, H.; Terracol, S.; Kahn, S.M.; Szymkowiak, A.E. The Astro-E2 X-ray spectrometer/EBIT microcalorimeter X-ray spectrometer. *Rev. Sci. Instrum.* **2004**, *75*, 3772–3774.
56. Porter, F.S.; Beck, B.R.; Beiersdorfer, P.; Boyce, K.R.; Brown, G.V.; Chen, H.; Gygax, J.; Kahn, S.M.; Kelley, R.L.; Kilbourne, C.A.; *et al.* The XRS microcalorimeter spectrometer at the Livermore electron beam ion trap. *Can. J. Phys.* **2008**, *86*, 231–240.
57. Osborne, G.C.; Safronova, A.S.; Kantsyrev, V.L.; Safronova, U.I.; Beiersdorfer, P.; Williamson, K.; Weller, M.E.; Shrestha, I. Spectroscopic Analysis and Modeling of Tungsten EBIT and Z-Pinch Plasma Experiments. *Can. J. Phys.* **2011**, *89*, 599–608.
58. Beiersdorfer, P.; Magee, E.W.; Brown, G.V.; Hell, N.; Träbert, E.; Widmann, K. Extended-range grazing-incidence spectrometer for high-resolution extreme ultraviolet measurements on an electron beam ion trap. *Rev. Sci. Instrum.* **2014**, *85*, 11E422.
59. Sugar, J.; Kaufman, V. Seventh spectrum of tungsten (W vii); resonance lines of Hf v. *Phys. Rev. A* **1975**, *12*, 994–1012.
60. Ryabtsev, A.N.; Kononov, E.Y.; Kildiyarova, R.R.; Tchang-Brillet, W.Ü.L.; Wyart, J.F. The spectrum of seven times ionized tungsten (W VIII) relevant to tokamak divertor plasmas. *Phys. Scr.* **2013**, *87*, 045303.
61. Beiersdorfer, P.; Bitter, M.; Roquemore, L.; Lepson, J.K.; Gu, M.F. Grazing-incidence spectrometer for soft X-ray and extreme ultraviolet spectroscopy on the National Spherical Torus Experiment. *Rev. Sci. Instrum.* **2006**, *77*, 10F306.
62. Graf, A.T.; Brockington, S.; Horton, R.; Howard, S.; Hwang, D.; Beiersdorfer, P.; Clementson, J.; Hill, D.; May, M.; Mclean, H.; *et al.* Spectroscopy on magnetically confined plasmas using electron beam ion trap spectrometers. *Can. J. Phys.* **2008**, *86*, 307–313.
63. Beiersdorfer, P.; Lepson, J.K.; Bitter, M.; Hill, K.W.; Roquemore, L. Time-resolved X-ray and extreme ultraviolet spectrometer for use on the National Spherical Torus Experiment. *Rev. Sci. Instrum.* **2008**, *79*, 10E318.
64. Clementson, J.; Beiersdorfer, P.; Gu, M.F.; McLean, H.S.; Wood, R.D. EUV spectroscopy on the SSPX spheromak. *J. Phys. Conf. Ser.* **2008**, *130*, 012004.

65. Lepson, J.; Beiersdorfer, P.; Clementson, J.; Bitter, M.; Hill, K.W.; Kaita, R.; Skinner, C.H.; Roquemore, L.; Zimmer, G. High-resolution time-resolved extreme ultraviolet spectroscopy on NSTX. *Rev. Sci. Instrum.* **2012**, *83*, 10D520.
66. Widmann, K.; Beiersdorfer, P.; Magee, E.W.; Boyle, D.P.; Kaita, R.; Majeski, R. High-resolution grazing-incidence grating spectrometer for temperature measurements of low-Z ions emitting in the 100–300 Å spectral band. *Rev. Sci. Instrum.* **2014**, *85*, 11D630.
67. Podpaly, Y.A.; Rice, J.E.; Beiersdorfer, P.; Reinke, M.L.; Clementson, J.; Barnard, H.S. Tungsten measurement on Alcator C-Mod and EBIT for future fusion reactors. *Can. J. Phys.* **2011**, *89*, 591–597.
68. Chowdhuri, M.B.; Morita, S.; Goto, M.; Nishimura, H.; Nagai, K.; Fujioka, S. Line analysis of EUV spectra from molybdenum and tungsten injected with impurity pellets in LHD. *Plasma Fusion Res.* **2008**, *2*, S1060.
69. Gu, M.F. The flexible atomic code. *Can. J. Phys.* **2008**, *86*, 675–689.
70. Clementson, J.; Beiersdorfer, P.; Brage, T.; Gu, M.F. Atomic data and theoretical X-ray spectra of Ge-like through V-like W ions. *At. Data Nucl. Data Tables* **2014**, *100*, 577–649.
71. Safronova, U.I.; Safronova, A.S.; Beiersdorfer, P. Dielectronic recombination and satellite line spectra of highly charged tungsten ions. *Can. J. Phys.* **2011**, *89*, 581–589.
72. Safronova, U.I.; Safronova, A.S.; Beiersdorfer, P.; Johnson, W.R. Excitation energies, radiative and autoionization rates, dielectronic satellite lines, and dielectronic recombination rates for excited states of Ag-like W from Pd-like W. *J. Phys. B At. Mol. Phys.* **2011**, *44*, 035005.
73. Safronova, U.I.; Safronova, A.S.; Beiersdorfer, P. Relativistic atomic data for Cu-like tungsten. *Phys. Rev. A* **2012**, *86*, 042510.
74. Safronova, U.I.; Safronova, A.S.; Beiersdorfer, P. Excitation energies, radiative and autoionization rates, dielectronic satellite lines, and dielectronic recombination rates for excited states of Yb-like W. *J. Phys. B At. Mol. Phys.* **2012**, *45*, 085001.
75. Safronova, U.I.; Safronova, A.S.; Beiersdorfer, P. Relativistic many-body calculations of excitation energies, oscillator strengths, transition rates, and lifetimes in samarium like ions. *Phys. Rev. A* **2013**, *87*, 032508.
76. Safronova, U.I.; Safronova, A.S.; Beiersdorfer, P. Contribution of the 4f-core-excited states in determination of atomic properties in the promethium isoelectronic sequence. *Phys. Rev. A* **2013**, *88*, 032512.
77. Safronova, U.I.; Safronova, A.S.; Beiersdorfer, P. Dielectronic recombination of Zn-like W^{44+} from Cu-like W^{45+} . *Phys. Rev. A* **2015**, submitted.
78. Seon, C.R.; Choi, S.H.; Cheon, M.S.; Pak, S.; Lee, H.G.; Biel, W.; Barnsley, R. Development of two-channel prototype ITER vacuum ultraviolet spectrometer with back-illuminated charge-coupled device and microchannel plate detectors. *Rev. Sci. Instrum.* **2010**, *81*, 10E508.
79. Beiersdorfer, P.; Brown, G.V.; Graf, A.T.; Bitter, M.; Hill, K.W.; Kelley, R.L.; Kilbourne, C.A.; Leutenegger, M.A.; Porter, F.S. Rest-wavelength fiducials for the ITER core imaging X-ray spectrometer. *Rev. Sci. Instrum.* **2012**, *83*, 10E111.

80. Beiersdorfer, P.; Clementson, J.; Widmann, K.; Bitter, M.; Hill, K.W.; Johnson, D.; Barnsley, R.; Chung, H.K.; Safronova, U.I. ITER core imaging X-ray spectroscopy: Atomic physics issues. *AIP Conf. Proc.* **2015**, *48*, 144017.
81. Beiersdorfer, P. Highly Charged Ions in Magnetic Fusion Plasmas: Research Opportunities and Diagnostic Necessities. *J. Phys. B* **2015**, in press.
82. Beiersdorfer, P.; Osterheld, A.L.; Chen, M.H.; Henderson, J.R.; Knapp, D.A.; Levine, M.A.; Marrs, R.E.; Reed, K.J.; Schneider, M.B.; Vogel, D.A. Indirect X-ray line formation processes in highly charged barium. *Phys. Rev. Lett.* **1990**, *65*, 1995–1998.
83. Chung, H.K.; Bowen, C.; Fontes, C.J.; Hansen, S.B.; Ralchenko, Y. Comparison and analysis of collisional-radiative models at the NLTE-7 workshop. *High Energ. Dens. Phys.* **2013**, *9*, 645–652.

© 2015 by the authors; licensee MDPI, Basel, Switzerland. This article is an open access article distributed under the terms and conditions of the Creative Commons Attribution license (<http://creativecommons.org/licenses/by/4.0/>).